Bidirectional shift in the cornu ammonis 3 pyramidal dendritic organization following brief stress

Kole, MHP; Costoli, T; Koolhaas, JM; Fuchs, E

Published in:
Neuroscience

DOI:
10.1016/j.neuroscience.2004.02.014

Publication date:
2004

Neuroscience 125 (2004) 337–347

BIDIRECTIONAL SHIFT IN THE CORNU AMMONIS 3 PYRAMIDAL DENDRITIC ORGANIZATION FOLLOWING BRIEF STRESS

M. H. P. KOLE,[a,b]* T. COSTOLI,[d] J. M. KOOLHAAS[c] AND E. FUCHS[a]

[a]*Clinical Neurobiology Laboratory, German Primate Center, Göttingen, Germany*

[b]*School of Behavioural and Cognitive Neurosciences, University of Groningen, Groningen, The Netherlands*

[c]*Laboratory of Animal Physiology, University of Groningen, Groningen, The Netherlands*

[d]*Dipartimento di Biologia Evolutiva e Funzionale, Sezione Fisiologia, Università di Parma, Parma, Italy*

Abstract—The negative impact of chronic stress at the structure of apical dendrite branches of cornu ammonis 3 (CA3) pyramidal neurons is well established. However, there is no information available on the CA3 dendritic organization related to short-lasting stress, which suffices to produce long-term habituation or sensitization of anxiety behaviors and neuroendocrine responses. Here, we tested the effects evoked by brief stress on the arrangements of CA3 pyramidal neuron dendrites, and the activity-dependent properties of the commissural-associational (C/A) excitatory postsynaptic potentials (EPSPs). Adult male rats were socially defeated followed by 3 weeks without further treatment or as comparison exposed to a regimen of a social defeat every second day for the same time period. We assessed CA3 pyramidal neurons with somatic whole-cell recording and neurobiotin application in acute hippocampal slices. The results from morphometric analysis of post hoc reconstructions demonstrated that CA3 dendrites from repeatedly stressed rats were reduced in surface area and length selectively at the apical cone (70% of control, approximately 280 μm from the soma). Brief stress, however, produced a similar decrease in apical dendritic length (77% of control, approximately 400 μm from the soma), accompanied by an *increased* length (167% of control) and branch complexity at the basal cone. The structural changes of the dendrites significantly influenced signal propagation by shortening the onset latency of EPSPs and increasing input resistance (r=0.45, P<0.01), of which the first was significantly changed in repeatedly stressed animals. Both brief and repeated stress long-lastingly impaired long-term potentiation of C/A synapses to a similar degree (P<0.05). These data indicate that the geometric plasticity of CA3 dendrites is dissociated from repetition of aversive experiences. A double social conflict suffices to drive a dynamic reorganization, by site-selective elimination and de novo growth of dendrite branches over the course of weeks after the actual experience.

Key words: patch-clamp, EPSP, LTP, social stress, intracellular labeling, remodeling.

In the hippocampus, a structure being part of the limbic circuit strongly implicated in the stress response, the subfield of the hippocampus, cornu ammonis 3 (CA3) pyramidal dendrites transiently regress in branch length following daily repeated stress over the course of 3 weeks (Magariños and McEwen, 1995; Sousa et al., 2000; for review see McEwen, 1999). However, the conceptual interpretation of these findings still lacks consistency, which in part might depend on methodological and technical aspects of the studies.

First, although geometrical changes of the CA3 structure are considered to develop as a function of stress duration (McEwen, 1999), to our knowledge, no study has investigated animals with a long time delay after stress. This is a crucial issue since evidence is merging that several stress-induced alterations develop independent of the frequency or number of stressor repetitions but rather autonomously with the passage of time over the course of days or weeks (Koolhaas et al., 1997; Dal-Zotto et al., 2002). For example, a single stress episode suffices to induce long-term anxiety behaviors in response to novel stressors (Koolhaas et al., 1990; van Dijken et al., 1992). Also particularly well studied is the post stress development of the hypothalamic–pituitary–adrenal axis. A brief stress leads to both progressive sensitization toward novel mild stressors weeks later (Liberzon et al., 1999; Buwalda et al., 2001; Martí et al., 2001) or conversely, a desensitization to the same test stimulus (Martí et al., 2001; Dal-Zotto et al., 2002; Vallès et al., 2003). It might be hypothesized that such long-lasting behavioral adaptations require enduring modifications of the dendritic architecture of central neurons of the limbic system.

Secondly, all previous investigations of the CA3 dendrite-stress interactions have relied on comparative analyses of Golgi-impregnated hippocampal cells. Besides the capriciousness inherent to the technique, it underestimates qualitatively and quantitatively the dendritic structure and excludes analysis of the far distal branches (for discussion, see Ishizuka et al., 1995; Pyapali et al., 1998). Indeed, the sampling of CA3 cells is mostly confined to the CA3c region where the distal dendrites are smaller and less differentiated in apical structure (Li et al., 1994; Turner

*Correspondence to: M. H. P. Kole, Division of Neuroscience, John Curtin School of Medical Research, Australian National University, Canberra, ACT 0200, Australia. Tel: +1-61-2-6125-8927; fax: +1-61-2-6125-2687.
E-mail address: maarten.kole@anu.edu.au (M. H. P. Kole).

Abbreviations: ACSF, artificial cerebrospinal fluid; ANOVA, analysis of variance; AVP, arginin–vasopressin; CA3, subfield of the hippocampus, cornu ammonis 3; C/A, commissural–associational; DAB, 3′,3-diaminobenzidine tetrahydrochloride; EPSP, excitatory postsynaptic potential; IO, input–output; IR-DIC, infrared–differential interference contrast; LSD, least significant difference; LTD, long-term depression; LTP, long-term potentiation; NMDA, *N*-methyl-D-aspartate; PB, phosphate buffer; PVN, paraventricular nucleus.

0306-4522/04$30.00+0.00 © 2004 IBRO. Published by Elsevier Ltd. All rights reserved.
doi:10.1016/j.neuroscience.2004.02.014

et al., 1995; Ishizuka et al., 1995). Therefore, to test whether dendrites are affected in their entire apical structure, including the lacunosum-moleculare, the visualization of intracellular labeled pyramidal neurons might provide a better alternative and facilitate the examination of fine distal dendrites (Horikawa and Armstrong, 1988; Amaral et al., 1990; Ishizuka et al., 1995; Pyapali et al., 1998).

In the present study we tested the hypothesis that brief stress suffices to induce transient or permanent changes in the dendritic patterns. For these reasons, we examined the CA3 dendritic structure of adult male rats exposed to two social defeat stressors (Meerlo et al., 1996; Koolhaas et al., 1997). The changes in reward and anxiety behaviors and neuroendocrine responses induced with this paradigm have been reported previously (Koolhaas et al., 1990; Meerlo et al., 1996; Buwalda et al., 1999, 2001; von Frijtag et al., 2001). Here, we studied by somatic whole-cell recording of CA3 pyramidal cells in acute hippocampal slices the CA3 neurons and examined properties of the excitatory postsynaptic potentials (EPSPs) of the recurrent commissural–associational (C/A) collaterals, combined with intracellular staining. This approach allowed us also to characterize the influence of variability in dendrite structure on synaptic voltage propagation. The results evoked by two social conflicts were compared with those induced by an intermittent social defeat stress over the course of 3 weeks.

EXPERIMENTAL PROCEDURES

Animals and housing

Male Wistar rats (Harlan-Winkelmann, Borchen, Germany) were housed in groups of four animals per cage ($39\times23\times15$ cm^3) with food and water *ad libitum*. Animals were acclimatized for 2 weeks before the start of the experiment and kept under reversed light/dark conditions (lights on 21:00–09:00 h) and at a room temperature of 21 ± 1 °C. Resident rats (wild-type strain; Haren, University of Groningen, Groningen, The Netherlands) were housed in pairs of one male and one sterilized female in large plastic cages ($60\times40\times40$ cm^3=l×w×h) located in a separate room. All manipulations were performed during the rats' active period, between 13:00 h and 15:00 h (during the dark phase), under supplementary dim red light (<1 lux). Animal experiments were conducted in accordance with the European Council Directive of November 24, 1986 (86/609/ECC), and approved by the Government of Lower Saxony, Germany. We used the minimum number of animals required to obtain consistent data, and minimized animal suffering.

Stress procedure

Social defeat, a natural stressor for the rat, was achieved as described previously (Meerlo et al., 1996; Buwalda et al., 1999). In brief, before the start of the defeat procedure, the female wild-type rat was removed from the cage. Subsequently, the experimental male Wistar rat (intruder) was transferred from its group and introduced into the resident's cage. In typically less than a minute, the intruder rat was attacked by the male resident, after which it adopted freezing and submissive postures. For the remaining hour, the intruder was enclosed in a small wire-mesh compartment ($25\times15\times8$ cm^3) within the resident's cage. Thus, the intruder animals were protected from direct physical contact, but remained in olfactory, visual, and auditory contact with the resident male rat. Afterward, the intruder animal was housed singly until the electrophysiological experiments. Control and defeated animals were housed in the same room to rule out differential spatial clues (Lee and Kesner, 2002). In all cases, the intruder animal was defeated by the resident male rat.

Two different stress paradigms were applied (see Fig. 1A, B). One group of rats was defeated on 2 consecutive days and left singly housed for a total of 21 days (*brief stress*; $N=9$; Fig. 1A). Control animals ($N=10$) were subjected to similar handling procedures and transferred to a novel cage with sawdust bedding for 1 h on 2 consecutive days and remained, similar to the defeated animals, singly housed for a total of 21 days.

In a second series of experiments, rats were exposed to social defeat on every second day, for a period of 21 days, equivalent to 11 defeats (*repeated stress*; $N=4$; Fig. 1B). Control animals ($N=4$) were subjected to similar handling procedures and transferred to a novel cage with sawdust bedding for 1 h on the 11 experimental days and remained also singly housed.

Hippocampal slice preparation

In the morning of day 22, between 10:00 and 11:00 h, animals were weighed, deeply anesthetized with (in mg/kg body weight): 50 ketamine, 10 xylazine, and 0.1 atropine, using i.p. injection, after which animals were transcardially perfused with ice-cold carbogenated (95% O_2/5% CO_2) sucrose-based artificial cerebrospinal fluid (ACSF) solution. Sucrose–CSF contained (in mM) 206 sucrose, 1 $MgCl_2$, 2.5 KCl, 2 $MgSO_4$, 1.25 Na_2HPO_4, 26 $NaHCO_3$, 14 day-glucose, 1 kynurenic acid, 1.5 $CaCl_2$, 1 l(+)-ascorbic acid. This pre-perfusion (i) removes red blood cells that might interfere with the histological peroxidase reaction and (ii) enhances the viability of CA3 neurons (Aghajanian and Rasmussen, 1989; Kapur et al., 1998). The brain was rapidly removed and transverse 400-μm hippocampal slices were cut with a vibroslicer (Vibracut 2; FTB, Bensheim, Germany). Slices were stored in a carbogenated-ACSF-containing chamber at 33 °C for 1 h and afterward maintained at room temperature. ACSF for slice storing consisted of (in mM) 125 NaCl, 2.5 KCl, 1.25 Na_2HPO_4, 2 $MgSO_4$, 26 $NaHCO_3$, 1.5 $CaCl_2$, 1 l(+)-ascorbic acid, 14 D(+)-glucose, at 300 mOsm (all chemicals from Merck, Darmstadt, Germany). The adrenal glands were weighed immediately after the animals were killed, using an analytical balance.

Patch-clamp recording

The entorhinal–hippocampal area was dissected from the slice and transferred to a submerged type of recording chamber with continuously oxygenated ACSF (flow rate: 1–2 ml/min). Cell bodies and their proximal segments were visualized by infrared–differential interference contrast (IR-DIC) video microscopy with an upright microscope (Axioskop 2 FS; Zeiss, Göttingen, Germany) equipped with an ×40/0.80 W objective (Zeiss IR-Acroplan). To reduce any location-dependent variation in morphology (Ishizuka et al., 1995), only pyramidal-shaped somata inside the CA3 stratum pyramidale and located slightly distant from the tip of the hippocampal fissure (approximately CA3b) were used for recording. Post hoc visualization of labeled neurons verified this location (Fig. 2). Patch-clamp recording was performed using borosilicate glass pipettes with 3–5 MΩ resistance, connected to an Axopatch 200B amplifier (Axon Instruments, Union City, CA, USA), and PULSE software (HEKA, Lambrecht, Germany). The intracellular patch solution contained (in mM) 120 $KMeSO_4$ (ICN, Eschwege, Germany), 20 KCl, 10 HEPES, 0.2 EGTA, 2 Mg^{2+}-ATP, 10 phosphocreatine, and 0.3 Tris–GTP (Sigma-Aldrich, Steinheim, Germany), adjusted to pH 7.3 with KOH and to 290 mOsm. Data were collected by low-pass Bessel filtering at 5.0 kHz and further digitized and stored at 50 kHz using an ITC-16 computer interface (Instrutech Corporation, Port Washington, NY, USA) and PULSE software (v. 8.11; HEKA). In whole-cell current-clamp mode, the 'fast clamp' amplifier circuit was

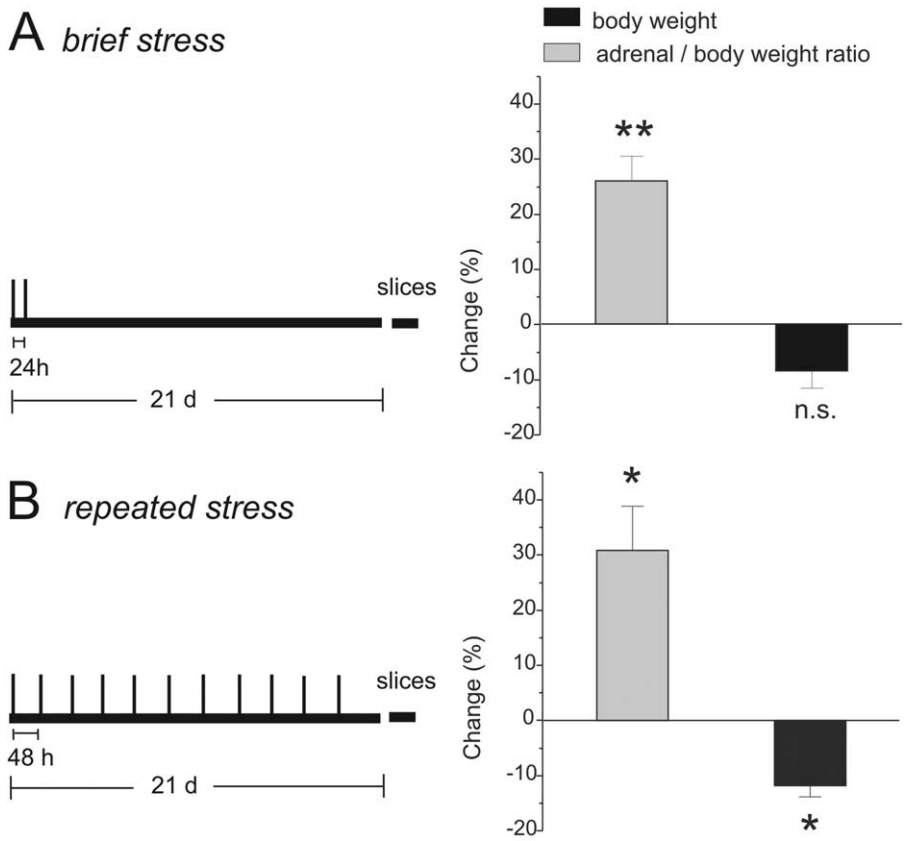

Fig. 1. Graphical representation of time and treatment frequency for the two experimental paradigms. (A) Brief stress was performed by exposing rats (N=9) to a standard social defeat paradigm (1 h) on 2 consecutive days. After the initial social stress, animals were left isolated and not handled until they were killed on day 22. Control animals (N=10) were handled in the same manner but transferred into a similar cage with sawdust only. The agonistic interactions led to an increase in the adrenal to body weight ratio ($P<0.0001$) and a slight non-significant decrease in body weight ($P<0.10$) compared with control. See Results for further data. (B) The repeated-stress paradigm consisted of a protocol in which rats (N=4) were exposed to the social stress paradigm on an intermittent basis, by 48 h, for 11 social defeat exposures. As in the brief-stress protocol, the animals were killed on day 22 after the first stress experience and standard hippocampal slices were prepared. Control animals (N=4) were handled in the same manner but transferred into similar large cages with sawdust. The intermittent stress had significant effects on body weight and adrenal weights ($P<0.05$ for both).

used, and both bridge voltage and series resistance (<12 MΩ) were continuously monitored and corrected when appropriate.

Tungsten electrodes (0.1 MΩ) were used to electrically stimulate C/A fibers. Because the distance between C/A axon stimulation and the cell-body recording site determines the rise-time kinetics of the EPSP (4.1 ms at <200 μm, and 5.6 ms at >200 μm; Kapur et al., 1998), we standardized the placing of the electrode at approximately 300 μm distal and 100 μm lateral to the recording electrode. In current-clamp, the cells were held close to −75 mV, approximating the type A GABA reversal potential, and C/A EPSPs were collected at a basal frequency of 0.05 Hz. EPSPs were isolated by blocking $GABA_A$-mediated activity with 10 μM (−)-bicuculline methobromide and 50 μM picrotoxin (Tocris, Bristol, UK). To test for plasticity, EPSPs were evoked and recorded at a basal frequency of 0.05 Hz for 8 min and then shortly potentiated by applying a mild low-frequency paradigm of 3 Hz for 3 min. All data were collected at 32±2 °C.

Labeling of identified neurons

All neurons were intracellularly labeled (Horikawa and Armstrong, 1988) with 3 mg/ml Neurobiotin (Vector Laboratories Inc., Wertheim, Germany), added to the patch solution. After recording, the patch-pipettes were carefully withdrawn from the membrane and the slices were fixed in 0.1 M phosphate buffer (PB) with 4% paraformaldehyde (pH 7.4) and stored at 4 °C for 2 days. Whole slices were processed, floating in wells, by first removing endogenous peroxidase activity in a 0.1 M PB solution containing 2% H_2O_2. They were subsequently rinsed with an avidin–biotin peroxidase solution (diluted 1:100; ABC; Vector Laboratories) with 1% bovine serum albumin (Sigma) and 0.3% Triton X-100, and stored for 24 h at 4 °C. Slices were washed several times in fresh 0.1 M PB and then treated with a PB solution containing 0.04% 3′,3-diaminobenzidine tetrahydrochloride (DAB; Vector Laboratories) and 0.002% NiH_4SO_4 for 20 min. This was immediately followed by incubation in a second freshly prepared DAB solution with 0.001% H_2O_2 until dark brown staining appeared, in typically less than 10 min. The reaction was terminated by several washings in fresh 0.1 M PB and distilled water. Tissue sections were dehydrated in an ascending series of ethanol, cleared in xylene, and flat-embedded in Eukitt (Kindler, Freiburg, Germany) on glass slides. Slices from stressed and control animals were always processed simultaneously.

Neuronal reconstruction and morphometric analysis

Labeled cells were visualized with light microscopy and evaluated for staining-quality. The criteria for including cells for quantification were visibility up to the most distal apical dendrites, clear dense labeling of the processes and the absence of cell coupling, such that all dendrites could be assigned unequivocally to a single cell. The IR-DIC patch-clamp technique provides an excellent high

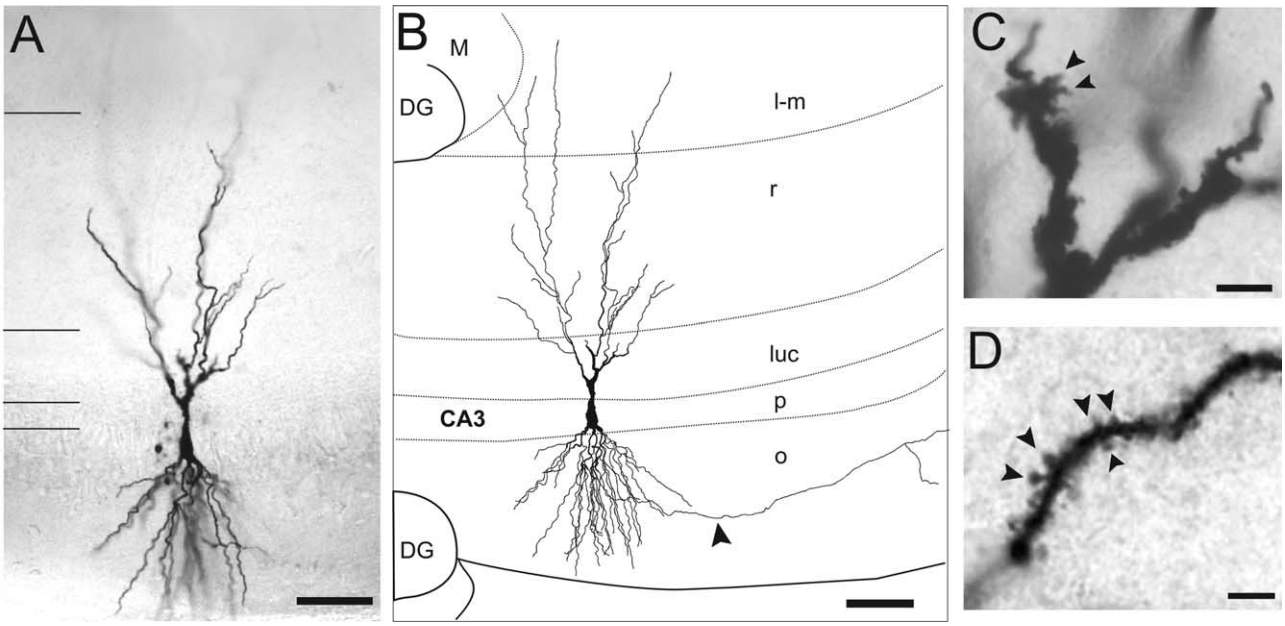

Fig. 2. Example of an intracellularly labeled and reconstructed CA3 pyramidal cell. (A) Photomicrograph of an intracellularly labeled CA3 pyramidal neuron from a briefly stressed rat. Note the highly polarized branch distribution, shifted from the apical toward the basal cone of the cell. Scale bar=100 μm. (B) Line-drawing of the same neuron shown in A, obtained by reconstruction with neurolucida. The arrowhead marks an axon running through the stratum oriens. The relative position of the CA3 pyramidal cell is given by lines indicating the various hippocampal layers. DG, dentate gyrus; l-m, lacunosum moleculare; luc, stratum lucidum; m, stratum moleculare; o, stratum oriens; p, stratum pyramidale; r, stratum radiatum. Scale bar=100 μm. (C) High-magnification photomicrograph of the thorny excrescences (indicated by arrowheads) of the same neuron. Scale bar=5 μm. (D) High-magnification photomicrograph of spines (arrowheads) located on an oblique branch within the stratum radiatum. Scale bar=4 μm.

signal-to-noise ratio for electrophysiological recordings, but restricts the approach of cell bodies to within 100 μm from the slice surface. Cells that were obviously defective in anatomical structure, with, for instance, severed main apical or basal dendrites were excluded from the analysis. The optimally labeled pyramidal neurons meeting all criteria were quantified for dendritic morphometry using NeuroLucida software (Microbrightfield Inc., Colchester, VT, USA) in combination with an automated stage and focus control connected to a microscope (Zeiss II RS).

The data were collected as line drawings consisting of *x*, *y*, and *z* coordinates, together with quantitative information on the dendritic diameter, by superimposing a circular cursor to the size of the dendrite. Dendritic length and surface measurements were made by tracing dendrites with a ×40 (N.A. 0.75) objective and final magnification at the monitor of ×40,000. Here, the step sizes of the circular cursor were 0.16 μm, sufficiently below the limits of light-microscopy resolution (approximately 0.25 μm). Numerical analysis and graphical processing of the neurons were performed with NeuroExplorer (v. 3.21; Microbrightfield). Sholl plots (Sholl, 1953) were constructed by plotting the summed dendritic length as a function of distance from the middle of the soma, set at zero, and dendrites summed in each subsequent radial bin of 20 μm.

Ethanol dehydration and xylene clearance causes tissue shrinkage (Pyapali et al., 1998). To estimate shrinkage in the *z* plane, the slice thickness was determined with the microscope micrometer, and by carefully monitoring the slice edges. A correction factor of 1.35 was applied to each plane, which is within the range of previously determined factors (Pyapali et al., 1998). For the ultimate comparison of between-subject effects, the linear shrinkage correction has no direct effect on the outcome or conclusions.

The use of uncut 400-μm slices greatly facilitates the reconstruction of the dendritic structure and length, but does not allow to resolve the anatomical fine structures, such as dendritic spines (see also Ishizuka et al., 1995; Henze et al., 1996) and fails to provide the complete neuron, as the axonal arborization cannot be reconstructed. Therefore, we did not attempt to quantitatively determine spine distribution or density, so the present measurements of surface area and volume should be accepted tentatively as estimates. When comparing basic numerical data with previously described CA3b pyramidal cell morphology the total dendritic length of the control cells, 9.7 mm, was on average only slightly less (11 mm in Henze et al., 1996 and Ishizuka et al., 1995).

Data analysis

Voltage recordings were only included for analysis when showing (i) a membrane potential of −55 mV or lower and (ii) a stable series resistance was measured for longer then 30 min. In long-term potentiation (LTP) experiments, the data were expressed as the percentage change in EPSP amplitude normalized to the average EPSP during the initial baseline period (100%). In the cumulative probability plots, all data points between 20 and 30 min after LTP establishment were averaged between animals and binned. Monoexponential fitting of EPSP decay was performed with PULSE-FIT (HEKA).

Analysis of variance (ANOVA) of data collapsed across neurons between control animals that were repeatedly handled or handled twice with a 3-week delay indicated that repeated handling had no effect per se on either body weight or adrenal weight ($P>0.06$), dendritic morphometry ($P>0.1$), or EPSP kinetics ($P>0.4$), which justifies the pooling of these data. Throughout this article, therefore, three groups are used: control, briefly stressed, and repeatedly stressed animals. The null hypothesis was explored by one-way ANOVA (SPSS v10.0; SPSS Inc., Chicago, IL, USA) followed by least significant difference (LSD) post hoc comparisons. Correlation analysis was performed with bivariate Pearson's correlation test. All significance levels were set to $P<0.05$.

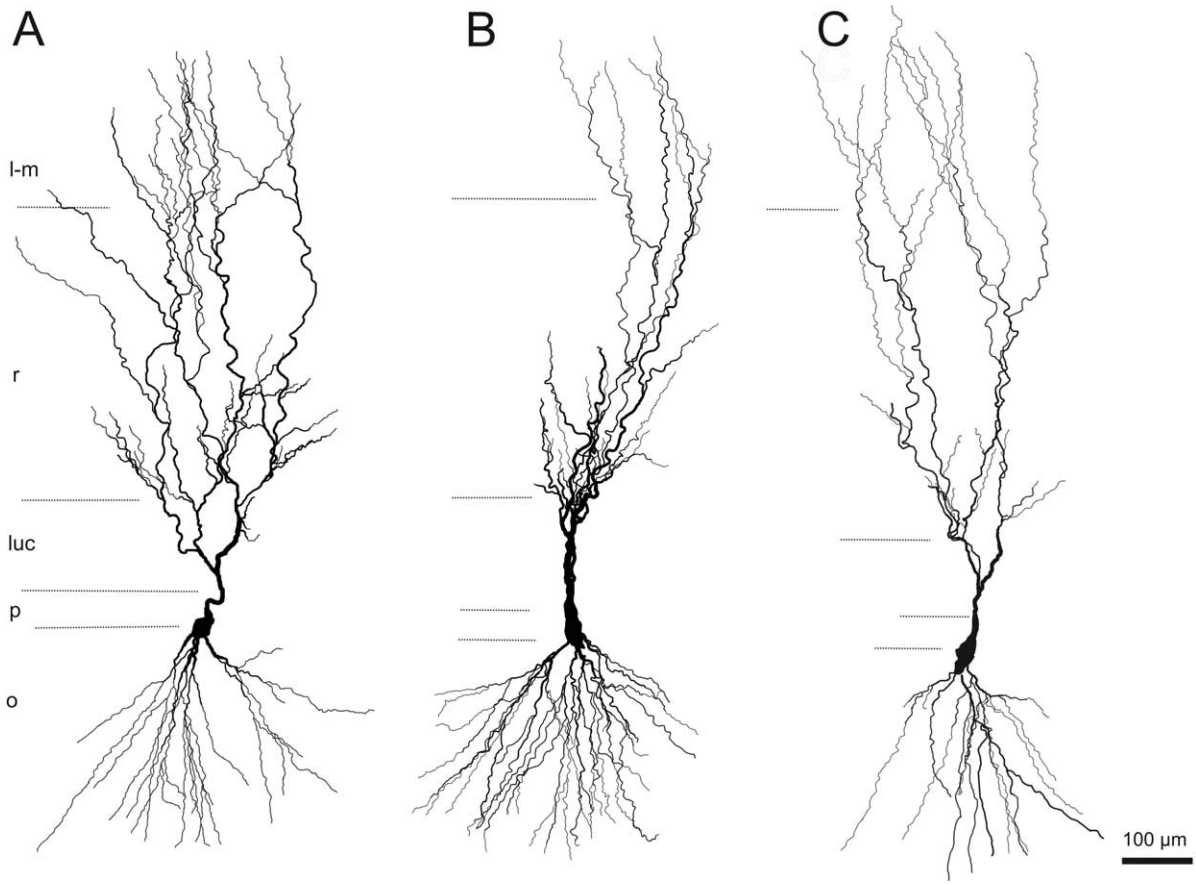

Fig. 3. Representative examples of neurolucida reconstructions of CA3 pyramidal neurons from each experimental group. (A) Control, (B) briefly stressed, and in (C), repeatedly stressed rats. Note the reduction in dendritic length on the apical side in cells of animals exposed to both type of stress regimens. A selective increase in basal branches occurred only in the CA3 neurons of briefly stressed rats. Numerical data of the dendrite reconstructions are presented in Table 1.

Graphical processing was done with Origin (v. 6.1; Microcal Software, Northampton, MA, USA). Data are given as means±S.E.M.

RESULTS

Effects of stress on body and adrenal weights

The exposure to social defeat affected the mean body and adrenal weights of the animals ($F_{2,26}=3.90$, $P<0.034$, and $F_{2,26}=12.50$, $P<0.001$, respectively; Fig. 1A, B). The exposure to brief stress elevated the total adrenal weight ($P<0.02$, $N=9$) as well as the adrenal to body weight ratio (stress: 13.77±0.44 g/100 g; control: 10.87±0.55 g/100 g; $P<0.0001$, $N=9$; Fig. 1A). The body weight, however, was only slightly reduced to approximately 90% of the control value at the end of the experimental period ($N=9$, $P<0.10$). The rats subjected to the repeated-stress paradigm (Fig. 1B) had a final mean body weight of 88.2±1.8% that of the controls (repeatedly stressed, 317.5±6.0 g; control, 280±5.8 g; post hoc test $P<0.015$; Fig. 1B) and in addition their adrenal to body weight ratios were also significantly increased (repeatedly stressed, 11.8±1.5 g/100 g; control, 9.0±0.3 g/100 g; $N=4$; $P<0.05$; Fig. 1B).

Therefore, the endpoint of adrenal-to-body-weight ratio changed to a similar degree after brief- and repeated-stress exposures, but with a slight additional effect insofar as there was a more pronounced reduction in body weight when the agonistic interaction was repeated.

Morphology of CA3 pyramidal neurons

For 36 of the 79 (47%) CA3 pyramidal cells examined in this study, the morphology could be recovered, allowing quantitative analysis of essential aspects of their dendritic structures (Fig. 2A–D). All CA3 neurons included in the analysis (the criteria are described in Experimental Procedures) were found to be located within the CA3b area (Ishizuka et al., 1995; Henze et al., 1996). Fig. 2 shows a neuron from a briefly stressed animal. The CA3 dendritic architecture consists of a low number of oblique branches, a maximum branch order of six to 11, thorny excrescences in the stratum lucidum (Fig. 2C), and spines located in the stratum radiatum (Fig. 2D). Examples of computer-assisted reconstructions for each group are given in Fig. 3A, B. The dendritic arborization was analyzed for numerical parameters of the soma, apical and basal dendrites. Table 1 lists the average values for each group.

Table 1. Morphometric data of CA3 pyramidal neuron dendrites of control, briefly and repeatedly stressed animals[a]

n	Control 16	Brief stress 12	Repeated stress 8	*P*
Soma perimeter (μm)	97.4±8.85	91.8±7.46	78.0±6.13	n.s.
Soma surface (μm^2)	216±11.2	264±20.4	236±11.1	n.s.
Trunk diameter (μm)	3.83±0.21	4.43±0.18*	3.49±0.27	0.04
Total tree				
Length (mm)	9.69±0.45	9.44±0.76	7.68±0.38	n.s.
Surface (mm^2)	25.9±1.90	26.8±2.62	17.6±1.51*§	0.03
Volume (mm^3)	8.61±0.96	9.19±0.10	5.12±0.73*§	0.04
Apical tree				
Length (mm)	7.47±0.50	5.73±0.72*	5.13±0.72*	0.03
Surface (mm^2)	21.2±1.85	17.7±2.23	12.6±1.72*	0.03
Volume (mm^3)	7.26±0.83	6.72±0.90	3.94±0.52*§	0.04
Nodes (#)	25.1±1.80	21.4±3.43	19.8±2.75	n.s.
Endings (#)	27.1±1.80	23.5±3.84	21.3±2.66	n.s.
Maximum branch order	8.88±0.47	8.67±0.67	8.63±0.71	n.s.
Basal tree				
Length (mm)	2.21±0.28	3.71±0.36*	2.56±0.31	0.005
Surface (mm^2)	4.70±0.61	9.05±1.04***	4.94±0.84§§	0.001
Volume (mm^3)	1.35±0.21	2.47±0.33**	1.26±0.25§§	0.006
Nodes (#)	10.8±1.50	19.0±2.01**	12.8±1.10§	0.003
Endings (#)	13.8±1.58	22.8±2.22**	16.6±1.36§	0.003
Maximum branch order	5.27±0.36	6.33±0.26*	4.63±0.32§	0.009

[a] The numerical average (mean±S.E.M.) of the morphometric parameters of cells from different experimental groups; *n* indicates the number of cells. *P* designates the significance level of one-way ANOVA, which was followed by LSD post hoc analysis. The significance levels are denoted by * $P<0.05$, ** $P<0.01$, and *** $P<0.001$ relative to controls and § $P<0.05$, §§ $P<0.01$ relative to briefly stressed rats; n.s., not significant.

In animals exposed to brief stress the total length of the apical dendrites was reduced (−23%, $P<0.05$; Fig. 3B and Table 1). Surprisingly, in contrast to the apical tree, the branches from the basal dendrites were increased in all aspects, including length, volume, and nodes (65–95% increase; LSD post hoc test, $P<0.05$ for all; see Table 1). Moreover, branch complexity, evaluated by the highest branch order, was significantly increased ($P<0.05$). In addition, we also detected an increase in apical trunk diameter ($P<0.05$). Importantly, despite the marked opposite changes in dendritic elements between the apical and basal cones, the summed dendritic length was similar compared with the control total dendritic length.

When social conflicts were repeated there was also a significant effect on CA3 morphology. There was a great reduction in total dendritic length and volume and surface area (approximately 40% reduction; Table 1, Fig. 3C), although not in the number of dendritic nodes. The changes in dendrites occurred selectively on the apical side of the neuron, where the dendritic branches were reduced in volume, surface area, and length (approximately 30–50% reduction, $n=8$). Repeated stress did not affect basal dendrites.

To evaluate the detailed distribution of dendritic processes across the various sublayers of the CA3 region, we created Sholl plots (Sholl, 1953) in which summed dendritic length is expressed as a function of distance from the soma in radial bins of 20 μm (Fig. 4A, B). Brief stress followed by single housing led to a branch-length decrease that occurred more distal from the apical tree, approximately 400–600 μm from the middle of the soma. Basal dendrites were increased in length between approximately 80 and 160 μm (Fig. 4A). Similar results were obtained when comparing the density of dendritic intersections as a function of radial distance (data not shown). It appeared that the reduction of dendritic elements after repeated stress was confined to the middle part of the apical tree, between approximately 280 and 340 μm from the soma (Fig. 4B).

Resting CA3 membrane properties and EPSP kinetics

The resting membrane properties of 59 CA3 pyramidal neurons were determined immediately after breakthrough in somatic whole-cell configurations, using current- or voltage-clamp recording within the linear range of the I–V curve and small voltage or current injections. The resting membrane potential was not affected by stress (control V_M: −73.6±1.5 mV, brief stress: −79.3±4.9 mV, repeated stress: −78.0±3.1 mV, $F_{2,23}=1.16$, $P>0.33$). The input resistance (R_N) did not differ in variance (control: 70.6±4.6 MΩ, $N=12$; brief stress: 79.3±4.8 MΩ, $N=8$; repeated stress: 88.0±7.9 MΩ, $N=4$; $F_{2,23}=2.16$, $P>0.14$, respectively). Also the slow-capacitances were similar between groups (200–215 pF; data not shown).

Upon stimulation of the C/A fibers and with inhibitory receptor blockers in the bath, somatically recorded EPSPs in control animals were quantified to establish their kinetics (Fig. 5A–D). In control recordings, the C/A EPSP responses, which are a composite of *N*-methyl-D-aspartate (NMDA) and α-amino-3-hydroxy-5-methyl-4-isoxazole propionate receptor-mediated potentials (Debanne et al., 1998; Urban et al., 2001), were characterized by 10–90%

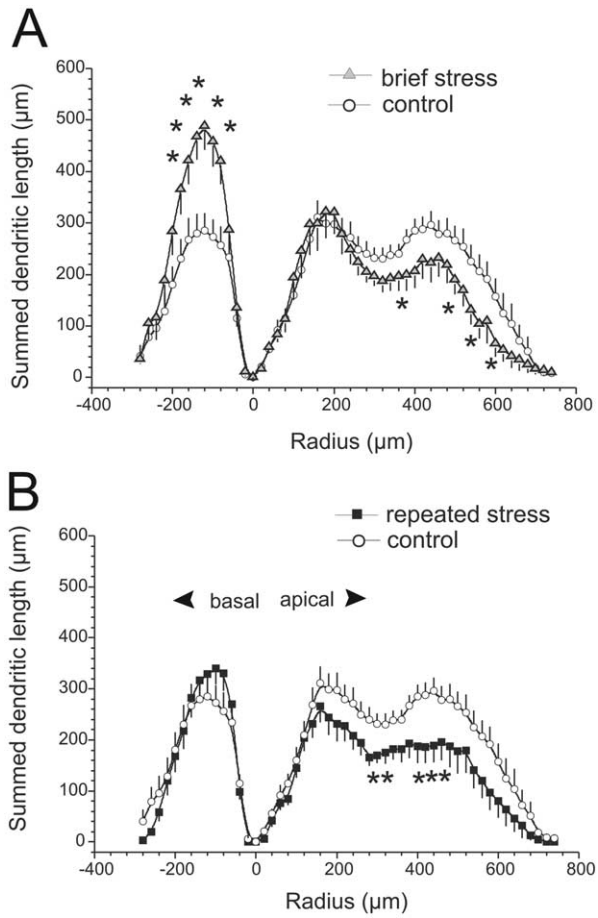

Fig. 4. Sholl analysis of the distance-dependent distribution of the apical and basilar dendrites. (A) Neurons from briefly stressed rats had shorter dendritic length within 400, 540, 560, and 600 μm from the soma (unpaired *t*-tests: $P<0.05$). Markedly increased length of basal dendrites was detected in the stratum oriens for the rings between 80 and 160 μm distance (unpaired *t*-tests: $P<0.01$). (B) Comparing control with repeatedly stressed animals shows that there is a reduction in CA3 dendritic length in the stratum radiatum for the rings 280, 300 and 380–440 μm from the soma (unpaired *t*-tests: $P<0.05$). No changes occurred in the basal dendrites. The dendritic length was summed in radii at 20 μm distance, with the middle of the soma set at zero. Apical dendrites are plotted to the right and basilar dendrites to the left as a function of distance from the soma center. Asterisks indicate significant difference ($P<0.05$) within each ring of 20 μm.

rise times of, on average, 4.7±0.19 ms (range 3.3–7.0 ms, $n=36$) which is consistent with a C/A origin, and is frequently used as a major indicator to distinguish mossy-fiber and C/A input (Kapur et al., 1998). Furthermore, the onset latency for the C/A EPSP was on average approximately 2.6 ms (range 1.9–3.8 ms), in agreement with previous data (2.7 ms in Kapur et al., 1998).

We compared the average rise and decay kinetics of C/A EPSPs between the three groups. The results indicate that only exposure to repeated stress altered the C/A EPSP kinetics (Fig. 5A, B). Here, the onset latency of the EPSP was reduced by 17% ($F_{2,23}=4.78$, $P<0.02$; Fig. 5A) and also the rise-time was shorter, compared with brief stress (repeated stress: 4.04±0.36 ms; brief stress: 5.45±0.40 ms; control: 4.63±0.26 ms; $F_{2,23}=3.32$, $P<0.056$). No changes were found in the decay times (approximately 34.2 ms in control and 37.3 ms in stress). Furthermore, across the linear range of the EPSP responses to varying stimulus strength, there was a clear effect on the input–output (IO) relation in the increased slope of the EPSPs (Fig. 5B, C; $F_{2,17}=4.69$, $P<0.05$). The repeatedly stressed animals had larger IO slope values than those of the control or briefly stressed animals (post hoc test, $P<0.05$ and $P<0.001$, respectively).

Morphological correlates of physiological parameters

Because the rise and decay kinetics of remote synaptic events are known to depend on dendritic structure (Henze et al., 1996; Golding et al., 2001; Vetter et al., 2001; reviewed in Spruston et al., 1999) we explored our whole-cell patch-clamp data from neurons that were morphologically reconstructed to test whether the stress-induced dendritic changes are involved in shaping the kinetics of the C/A EPSPs. Linear association analysis showed that the apical surface and length correlated with the value of the resting input resistance (R_N; $r=-048$, $P<0.01$, $n=32$). As expected, the R_N was also associated with the duration of EPSP decay kinetics ($r=0.43$, $P<0.01$, $n=32$; data not shown). The latency of onset of the C/A EPSP correlated significantly with the geometrical structure of the apical tree, in that a greater number of nodes or greater apical length resulted in a longer latency time ($r=0.45$, $P<0.006$, and $r=0.33$, $P<0.05$, respectively; $n=37$; Fig. 5D). This partly corresponds to the difference in physiology of the three groups: although the apical nodes were not significantly reduced in the repeatedly stressed animals, CA3 neurons from this group did have significantly less apical surface and also a smaller latency of EPSP. Aspects of the basal dendrites did not correlate with any physiological measurement.

Stress effects at C/A LTP

We tested further the prediction that stress would affect the LTP of the C/A CA3 synapses. During control baseline recording EPSPs were elicited from a membrane potential of −75 mV and scaled to amplitudes of approximately 6.5 mV (not different between groups, $P>0.9$) to obtain similar depolarization levels. As shown in Fig. 6A, in control animals, LTP was elicited by a brief low-frequency tetanic stimulation, 3 Hz for 3 min, which led to a gradual and progressive increase in the EPSP amplitudes, reaching 150% potentiation 20 min after frequency stimulation with high probability (Fig. 6A, B). The applied low-frequency 3-Hz tetanization of C/A synapses in control animals positively regulated the synaptic strength of the EPSPs, instead of inducing LTD (Chattarji et al., 1989; Debanne et al., 1998) probably since under current-clamp conditions the application of blockers for $GABA_A$-mediated receptor currents facilitates frequency-dependent disinhibition through the reduction of the driving force of chloride and the presynaptic inhibition of GABA release by $GABA_B$ receptor activation (Wigström and Gustafsson, 1983; Hsu et al., 1999; Kuenzi et al., 2000).

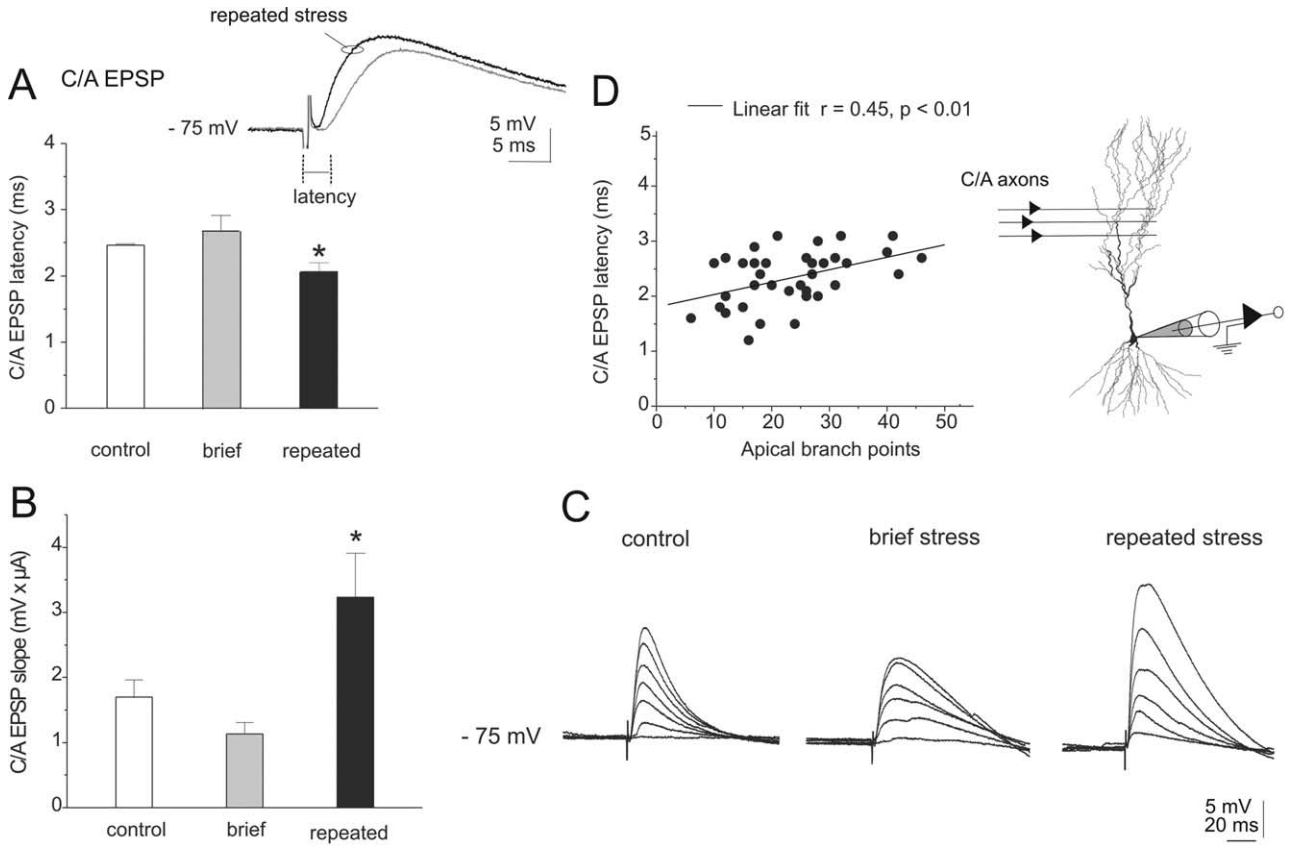

Fig. 5. Stress and dendrite geometry affect at the C/A EPSPs. (A) At the right is the whole-cell recording configuration of the CA3 pyramidal cell and site of stimulation depicted. The stimulation was fixed to approximately 300 μm from the soma to evoke C/A EPSPs. (B) Plot of the IO curves constructed for the C/A EPSP amplitudes. Repeated stress significantly increased the slope of the linear fit through the data points (repeated stress, approximately 3.1 mV μA relative to the control, 1.1 mV μA; $F_{2,17}=4.69$, $P<0.026$). Data are given as mean±S.E.M. (C) Examples of a family of EPSP responses elicited by varying stimulus intensities (1 μA steps) for each experimental group, from left to right: control, brief stress and repeated stress. (D) Apical dendritic geometrical structure, defined as the number of apical nodes, determines the latency of C/A EPSPs. Plotted are the onset latencies from the cells against their reconstructed number of nodes in the apical tree. The fitting derives from the linear correlation analysis of morphological data compared with the onset latency ($r=0.45$, $P<0.05$, $n=37$). Here, r indicates the Pearson's Rho correlation coefficient.

In slices from briefly stressed animals after a 21-day time delay, LTP could not be evoked (98.4±14.6%, $n=7$, $P<0.01$ compared with control LTP; Fig. 6B). In recordings from repeatedly stressed animals, low-frequency potentiation tended to reverse the EPSP amplitude, resembling long-term depression (LTD; 56% probability of 70% EPSP amplitude, Fig. 6B, C). The EPSPs showed a probability distribution similar to that of briefly stressed rats (Fig. 6C). While no differences were detectable between repeated and brief stress ($P>0.20$) these data show that the repetition does not result in more LTP suppression at C/A synapses.

DISCUSSION

We examined the CA3 pyramidal neurons from socially defeated rats 3 weeks after a distinct number of social conflicts. The combined approach of intracellular labeling and electrophysiological analysis of rat CA3 pyramidal neurons allowed us to evaluate novel qualitative and quantitative aspects of the stress-induced modifications, including the functional consequences.

Stress induces laminar-specific dendritic changes in CA3 dendritic arborization

Three weeks after a brief stress episode, a complex shift developed in the branching pattern of the CA3 pyramidal neurons: dendritic branches are added to the basal cone, but pruned in the apical tree. The elimination of apical branches occurred not homogenous across the dendritic tree, but was only observed approximately 400 μm from the soma, and further distal. However, despite the profound structural redistribution, the total surface area and dendritic length were preserved (Table 1, Fig. 4).

Also in the repeated defeat group we observed that the reduction of dendritic elements is not occurring equally across fine distal apical branches but affected within a confined spatial domain, most prominently between approximately 300 and 420 μm distance from the soma, approximating the associational zone of the CA3 field (Ishizuka et al., 1990, 1995). The most distal branches, however, where perforant-path input synapses at the CA3 cells, within the lacunosum-moleculare subfield, are preserved in length and number. These findings are sup-

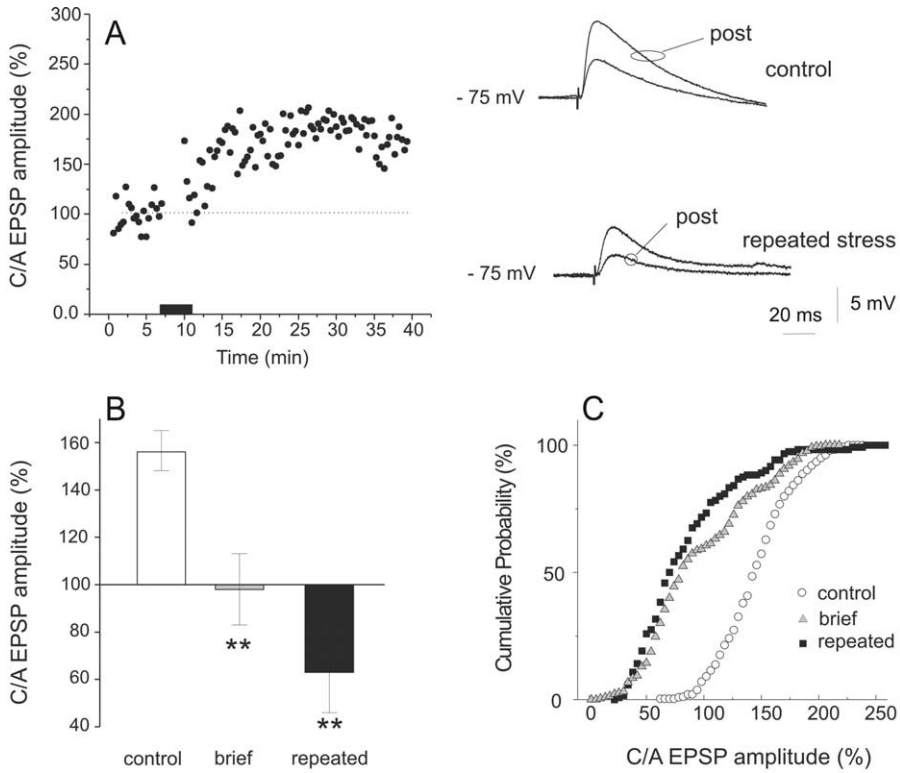

Fig. 6. Long-lasting bimodal regulation of social-stress stress on tetanic potentiation of the C/A synapse. (A) Scatter plots show the time development of EPSP potentiation, recorded at a frequency of 0.05 Hz. A short low-frequency stimulation of 3.0 Hz (3.5 min) induced a robust LTP-like potentiation at the C/A synapse in control animals with a mean amplitude change of 153.9±8.8%, $n=12$. At the right are examples given of C/A EPSPs traces before and after low-frequency stimulation. Below, an example from the repeated-stress group in which the same tetanic potentiation induced LTD of the CA/ synaptic strength. (B) Population data of the change in EPSPs amplitudes measured between 20 and 25 min after tetanic stimulation with respect to baseline amplitudes. The synaptic potentiation was significantly affected by stress ($F_{2,22}=7.81$, $P<0.003$). Animals exposed to a brief-stress paradigm with 3 weeks of single housing showed a mixed response to mild synaptic potentiation with a mean of 98.1±17.2% ($n=8$, $P<0.01$). However, in repeatedly stressed animals ($n=4$), a robust LTD-like EPSP depression (63.8±8.9%, $P<0.01$) was observed. Data are given as mean±S.E.M. (C) Cumulative probability curves constructed from the same data within the 20–25 min post-frequency potentiation. The cumulative probability for 130% LTP in control animals (*open circles*) was 40%, but for synaptic depression (70% amplitude) was only 1%. For the stressed animals, however, there was a 56% probability of a 70% EPSP amplitude in repeatedly stressed animals (*gray squares*), and 47% in briefly stressed animals (*closed pyramids*).

ported by recent observations of the laminar pattern of the CA3 dendritic changes after chronic stress in tree shrews (Kole et al., 2004) and corroborates anatomical data revealing volume reductions after chronic stress selectively in the CA3 radiatum field (Lucassen et al., 2001).

Functional correlates of the dendritic geometric changes of CA3 dendrites

An important question is whether such morphological adaptations lead to functional changes in synaptic integration or intrinsic properties. The major reorganization of dendrites of briefly stressed animals did not affect the amplitude and kinetics of glutamate-receptor-mediated transmission. This maintenance in the excitatory input from commissural and associational fibers might depend on the additional number of basal dendritic branches. These arbors receive most of their input from the fimbria and lateral septum (Amaral and de Witter, 1989) but C/A synapses can additionally target basal segments (Li et al., 1994) and providing thus additional postsynaptic sources when stimulating the C/A fibers. Alternatively, the lower number of available branches in the radiatum contains higher glutamate-receptor channel density.

The repetitive stress in contrast, leading to a clear net loss of dendritic length, showed enhanced excitability. This increased excitation partially derives from geometry-dependent changes. First, the size of the apical receptive field, parameterized in branch nodes or apical length was significantly associated with increased somatic R_N, and secondly, associated to a shortened latency of the evoked C/A EPSP (Fig. 6). Although the R_N did not reach a difference in variance between groups, the predicted shortening of the onset latency of C/A EPSPs was indeed apparent after repeated stress (Fig. 5). These empirical observations are supported by studies isolating the biophysical effects of apical dendritic morphological diversity with compartmental models (Golding et al., 2001; Vetter et al., 2001) and studies addressing the effects of dendritic pruning of CA3 pyramidal neurons (Krichmar et al., 2002; Narayanan et al., 2003). A third geometry-related change might include a significant increase in backpropagation of action potentials within the CA3 stratum radiatum (Nara-

yanan et al., 2003). Finally, another source of hyperexcitability after chronic stress might depend on the increased NMDA-receptor activity of C/A synapses (Kole et al., 2002) leading to slower deactivation kinetics of the postsynaptic currents.

Taken together, the net loss of dendritic arbors renders pyramidal cells from repetitively stressed rats more susceptible for generating seizure activity, which has been sparsely investigated in relation to stress, although reported recently (Pavlides et al., 2002).

Temporal dynamics of brief stressors

Whereas the repeated stress-induced dendritic regression is thought to develop as a function of the prolonged endogenously elevated corticosteroids and glutamate release (Magariños and McEwen, 1995; McEwen, 1999) it is unlikely that our observed bidirectional adaptation can be explained by similar processes. A brief social-stress episode increases free corticosterone during the first 5 h only, after which the plasma levels maintain within a normal range for at least 3 weeks (Buwalda et al., 1999, 2001; M. Kole, unpublished observations).

Our main finding that even brief stress, and not necessarily its recurrence, induces large-scale dendritic rearrangements has therefore significant implications. The observations are most consistent with the conceptual framework that the passage of time after a single territorial conflict, one of the most intense stressors for the male rat, is followed by dynamic and temporal alterations in neuroendocrine systems and behaviors (Koolhaas et al., 1997). For example, single stress reduces hippocampal glucocorticoid receptor binding and expression 3 weeks but not 1 week after a single episode of stress (Buwalda et al., 1999, 2001; Liberzon et al., 1999) a change that is also evident after 3 weeks of daily stressors (Meyer et al., 1998). Tilders et al. (2001) found that 2 weeks of chronic stress drives the corticotropin-releasing factor neurons in the hypothalamus from non-arginin–vasopressin (AVP)-producing phenotype toward the AVP-coproducing type, a typical hallmark of chronic stress. However, the switch in neurochemical profile was also observed with simply awaiting the passage of time of 2 weeks after a single stress exposure. Such time-dependent changes in the CNS might support slow-developing behavioral adaptations. For example, 3 weeks after a single stress exposure, enhanced corticosteroid feedback has been demonstrated with exposure to a homotypical stressor (Martí et al., 2001) which did not differ compared with the outcome of repeated exposures (Dal-Zotto et al., 2002) indicating a requirement of slow-developing cellular learning processes to distinguish between stressors.

The dense excitatory CA3 network is in a strategic position to perform such changes. First, it maintains putative trans-synaptic inhibitory connections with paraventricular nucleus neurons (PVN) to alter corticosterone responses (Jacobson and Sapolsky, 1991; Roozendaal et al., 2001). Indeed, the re-exposure to the same stressor 3 weeks later produces a reduced activation of PVN cells (Vallès et al., 2003). Secondly, the CA3 recurrent synapses have a unique function to store information about a one-time experience (Rolls, 1996; Nakazawa et al., 2003). The feed-forward associational fibers are implicated both in recall of neuronal representations by NMDA-receptors that support the reorganization (Rolls, 1996; Lee and Kesner, 2002; Nakazawa et al., 2003). Therefore, it is tempting to assume that the CA3 subfield retains memory traces concerning the stress experience. Such neural information might play a role in the cortical processing through which behavioral responses and adrenocortical feedback are funneled and might be inhibited or disinhibited, leading to a fine-tuning of the stress response.

CONCLUSIONS

We conclude from our data that a brief stress exposure is sufficient to induce long-term and site-specific adaptations in dendritic architecture and the excitatory synapses of the CA3 pyramidal neurons. While we observed no difference in the elimination of dendritic arbors at the *apical* cone, a general conclusion is the importance to discern between stress-repetition-dependent and time-dependent adaptations. In fact, our data support the formulation that the outcome of repetition of stress is a temporary suppression of the addition of new branches at the CA3 cell rather then a necessary condition to induce dendrite retractions. This is indeed in line with data that upon arrest of chronic stress growth of branches is rapidly re-established and normal branch lengths obtained (Sousa et al., 2000). Our data demonstrate furthermore that only the net loss of branches comprises a risk for neuronal hyperexcitability. However, the slow-developing structural sorting of dendritic branches might provide a neuroanatomical basis for persistent and time-dependent neuroendocrine and behavioral changes long after the actual stress experience.

REFERENCES

Aghajanian GK, Rasmussen K (1989) Intracellular studies in the facial nucleus illustrating a simple new method for obtaining viable motoneurons in adult rat brain slices. Synapse 3:331–338.

Amaral DG, De Witter MP (1989) The three-dimensional organization of the hippocampal formation: a review of anatomical data. Neuroscience 31:571–591.

Amaral DG, Ishizuka N, Claiborne B (1990) Neurons, numbers and the hippocampal network. Prog Brain Res 83:1–11.

Buwalda B, de Boer SF, Schmidt ED, Felszeghy K, Nyakas C, Sgoifo A, van der Vegt BJ, Tilders FJH, Bohus B, Koolhaas JM (1999) Long-lasting deficient dexamethasone suppression of hypothalamic-pituitary-adrenocortical activation following peripheral CRF challenge in socially defeated rats. J Neuroendocrinol 11:513–520.

Buwalda B, Felszeghy K, Horváth KM, Nyakas C, de Boer SF, Bohus B, Koolhaas JM (2001) Temporal and spatial dynamics of corticosteroid receptor down-regulation in rat brain following social defeat. Physiol Behav 72:349–354.

Chattarji S, Stanton PK, Sejnowksi TJ (1989) Commissural synapses, but not mossy fiber synapses, in hippocampal field CA3 exhibit associative long-term potentiation and depression. Brain Res 495: 145–150.

Dal-Zotto S, Martí O, Armario A (2002) Is repeated exposure to immobilization needed to induce adaptation of the hypothalamic-pituitary-adrenal axis? Influence of adrenal factors. Behav Brain Res 129:187–195.

Debanne D, Gähwiler BH, Thompson SM (1998) Long-term synaptic plasticity between pairs of individual CA3 pyramidal cells in rat hippocampal slice cultures. J Physiol 507:237–247.

Golding NL, Kath WL, Spruston N (2001) Dichotomy of action-potential backpropagation in CA1 pyramidal neuron dendrites. J Neurophysiol 86:2998–3010.

Henze DA, Cameron WE, Barrionuevo G (1996) Dendritic morphology and its effects on the amplitude and rise-time of synaptic signals in hippocampal CA3 pyramidal cells. J Comp Neurol 369:331–344.

Horikawa K, Armstrong WE (1988) A versatile means of intracellular labeling: injection of biocytin and its detection with avidin conjugates. J Neurosci Methods 25:1–11.

Hsu KS, Ho WC, Huang CC, Tasi JJ (1999) Prior short-term synaptic disinhibition facilitates long-term potentiation and suppresses long-term depression at CA1 hippocampal synapses. Eur J Neurosci 11:4059–4069.

Ishizuka N, Weber J, Amaral DG (1990) Organization of intrahippocampal projections originating from CA3 pyramidal cells in the rat. J Comp Neurol 295:580–623.

Ishizuka N, Cowan WM, Amaral DG (1995) A quantitative analysis of the dendritic organization of pyramidal cells in the rat hippocampus. J Comp Neurol 362:17–45.

Jacobson L, Sapolsky R (1991) The role of the hippocampus in feedback regulation of the hypothalamic-pituitary-adrenocortical axis. Endocr Rev 12:118–134.

Kapur A, Yeckel MF, Gray R, Johnston D (1998) L-Type calcium channels are required for one form of hippocampal mossy fiber LTP. J Neurophysiol 79:2181–2190.

Kuenzi FM, Fitzjohn SM, Moron RA, Collingridge GL, Seabrook GR (2000) Reduced long-term potentiation in hippocampal slices prepared using sucrose-based artificial cerebrospinal fluid. J Neurosci Methods 100:117–122.

Kole MHP, Swan L, Fuchs E (2002) The antidepressant tianeptine persistently modulates glutamate receptor currents of the hippocampal CA3 commissural-associational synapse in chronically stressed rats. Eur J Neurosci 16:807–816.

Kole MHP, Czéh B, Fuchs E (2004) Homeostatic maintenance in excitability of tree shrew hippocampal CA3 pyramidal neurons after chronic stress. Hippocampus, in press.

Koolhaas JM, Hermann PM, Kemperman C, Bohus B, van den Hoofdakker RH, Beersma DGM (1990) Single social defeat in male rats induces a gradual but long lasting behavioural change: a model of depression? Neurosci Res Comm 7:35–41.

Koolhaas JM, Meerlo P, De Boer SF, Strubbe JH, Bohus B (1997) The temporal dynamics of the stress response. Neurosci Biobehav Rev 21:775–782.

Krichmar JL, Nasuto SJ, Scorcioni R, Washington SD, Ascoli GA (2002) Effects of dendritic morphology on CA3 pyramidal cell electrophysiology: a simulation study. Brain Res 941:11–28.

Lee I, Kesner RP (2002) Differential contribution of NMDA receptors in hippocampal subregions to spatial working memory. Nat Neurosci 5:162–168.

Li X-G, Somogyi P, Ylinen A, Buzsáki G (1994) The hippocampal CA3 network: and in vivo intracellular labeling study. J Comp Neurol 339:181–208.

Liberzon I, López JF, Glagel SB, Vázquez DM, Young EA (1999) Differential regulation of hippocampal glucocorticoid receptor mRNA and fast feedback: relevance to post-traumatic stress disorder. J Neuroendocrinol 11:11–17.

Lucassen PJ, Vollmann-Honsdorf GK, Gleisberg M, Gzéh B, de Kloet EF, Fuchs E (2001) Chronic psychosocial stress differentially affects apoptosis in hippocampal subregions and cortex of the adult tree shrew. Eur J Neurosci 14:161–166.

Magariños AM, McEwen BS (1995) Stress-induced regression of apical dendrites of hippocampal CA3c neurons: comparisons of stressors. Neuroscience 69:83–88.

Martí O, Garcia A, Vellès A, Harbuz MS, Armario A (2001) Evidence that single exposure to aversive stimuli triggers long-lasting effects in the hypothalamus-pituitary-adrenal axis that consolidates with time. Eur J Neurosci 13:129–136.

McEwen BS (1999) Stress and hippocampal plasticity. Annu Rev Neurosci 22:105–122.

Meerlo P, Overkamp GJ, Daan S, Van Den Hoofdakker RH, Koolhaas JM (1996) Changes in behaviour and body weight following a single or double social defeat in rats. Stress 1:21–32.

Meyer U, Kruhøffer M, Flügge G, Fuchs E (1998) Cloning of glucocorticoid receptor and mineralocorticoid receptor cDNA and gene expression in the central nervous system of the tree shrew (Tupaia belangeri). Mol Brain Res 55:243–253.

Nakazawa K, Sun LD, Quirk MC, Rondi-Reig L, Wilson MA, Tonegawa S (2003) Hippocampal CA3 NMDA receptors are crucial for memory acquisition of one-time experience. Neuron 24:305–315.

Narayanan R, Narayan A, Chattarji S (2003) Computational analysis of the effects of chronic stress on hippocampal excitability: from neurons to network. Proc Soc Neurosci 192.5.

Pavlides C, Nivon LG, McEwen BS (2002) Effects of chronic stress on hippocampal long-term potentiation. Hippocampus 12:245–257.

Pyapali GK, Sik A, Penttonen M, Buzsáki G, Turner DA (1998) Dendritic properties of hippocampal pyramidal neurons in the rat: intracellular staining in vivo and in vitro. J Comp Neurol 391:335–352.

Rolls ET (1996) A theory of hippocampal function in memory. Hippocampus 6:601–620.

Roozendaal B, Phillips RG, Power AE, Brooke SM, Sapolsky RM, McGaugh JL (2001) Memory retrieval impairment induced by hippocampal CA3 lesions is blocked by adrenocortical suppression. Nat Neurosci 4:1169–1171.

Sousa N, Lukoyanov NV, Madeira MD, Almeida OFX, Paul-Barbosa MM (2000) Reorganization of the morphology of hippocampal neurites and synapses after stress-induced damage correlates with behavioral impairment. Neuroscience 97:253–266.

Spruston N, Stuart G, Häusser M (1999) Dendritic integration. In: Dendrites (Stuart G, Nelson S, Häusser M, eds), pp 231–260. Oxford: OUP.

Sholl DA (1953) Dendritic organization in the neurons of the visual and motor cortices of the cat. J Anat Physiol 87:387–406.

Tilders FJH, Schmidt ED, De Goeij DCE (2001) Phenotypic plasticity of CRF neurons during stress. Ann NY Acad Sci 39–52.

Turner DA, Li X-G, Pypapali GK, Ylinen A, Buzsáki G (1995) Morphometric and electrical properties of reconstructed hippocampal CA3 neurons recorded in vivo. J Comp Neurol 356:580–594.

Urban NN, Henze DA, Barrionuevo G (2001) Revisiting the role of the hippocampal mossy fiber synapse. Hippocampus 11:408–417.

Vallès A, Martí O, Armario A (2003) Long-term, effects of a single exposure to immobilization stress on the hypothalamic-pituitary-adrenal axis: transcriptional evidence for a progressive desensitization process. Eur J Neurosci 18:1353–1361.

van Dijken HH, van der Heyden JAM, Mos J, Tilders FJH (1992) Inescapable footshocks induce progressive and long-lasting behavioural changes in male rats. Physiol Behav 51:787–794.

Vetter P, Roth A, Häusser M (2001) Propagation of action potentials in dendrites depends on dendritic morphology. J Neurophysiol 85: 926–937.

von Frijtag JC, Kamal A, Reijmers LGJE, Schrama LH, van den Bos R, Spruijt BM (2001) Chronic imipramine treatment partially reverses the long-term changes of hippocampal synaptic plasticity in socially stressed rats. Neurosci Lett 309:153–156.

Wigström H, Gustafsson B (1983) Facilitated induction of hippocampal long-lasting potentiation during blockade of inhibition. Nature 301:603–604.

(Accepted 11 February 2004)